Contrast Enhancement Based on Layered Difference Representation of 2D Histograms

Chulwoo Lee, *Student Member, IEEE,* Chul Lee, *Member, IEEE,* and Chang-Su Kim, *Senior Member, IEEE*

***Abstract*—A novel contrast enhancement algorithm based on the layered difference representation of 2D histograms is proposed in this work. We attempt to enhance image contrast by amplifying the gray-level differences between adjacent pixels. To this end, we obtain the 2D histogram $h(k, k+l)$ from an input image, which counts the pairs of adjacent pixels with gray-levels k and $k+l$, and represent the gray-level differences in a tree-like layered structure. Then, we formulate a constrained optimization problem based on the observation that the gray-level differences, occurring more frequently in the input image, should be more emphasized in the output image. We first solve the optimization problem to derive the transformation function at each layer. We then combine the transformation functions at all layers into the unified transformation function, which is used to map input gray-levels to output gray-levels. Experimental results demonstrate that the proposed algorithm enhances images efficiently in terms of both objective quality and subjective quality.**

***Index Terms*—Image enhancement, contrast enhancement, histogram equalization, 2D histogram, layered difference representation, and constrained optimization.**

I. Introduction

In spite of recent advances in imaging technology, captured images often fail to preserve scene details faithfully or yield poor contrast ratios due to limited dynamic ranges. Contrast enhancement (CE) techniques can alleviate these problems and bring out hidden details. CE is an essential step in various image processing applications, such as digital photography, video communications, and visual surveillance, and a lot of researches have been made to develop efficient CE techniques.

Conventional CE techniques can be categorized into global and local approaches. A global approach derives a single transformation function, which maps input intensities to output intensities, and applies it to all pixels in an entire image. For example, the gamma correction based on the simple power law is a well-known CE technique. On the other hand, a local approach, *e.g.* [2]–[6], derives and applies the transformation function for each pixel adaptively according to the information in a local neighborhood. However, in general, a local approach demands higher computational complexity and its level of CE is harder to control. Therefore, being more stable, global CE techniques are more widely used in practical applications.

Histogram specification (HS) [7], which attempts to obtain the output histogram of a desired shape, is a global CE technique. However, there is no obvious choice for the desired histogram, since natural images exhibit significantly different histogram characteristics from one another. Thus, simple mathematical distributions, such as uniform, Gaussian, or exponential, are typically used as the desired histograms. Especially, when the uniform distribution is used, HS is referred to as histogram equalization (HE) [7]. HE is one of the most widely adopted techniques to enhance low contrast images due to its simplicity and effectiveness. However, it has some drawbacks, such as contrast over-stretching, noise amplification, or contour artifacts. Various researches have been made to overcome these drawbacks. For example, several algorithms [8]–[10] divide an input histogram into sub-histograms and equalize them independently to reduce the brightness change between input and output images. Also, histogram modification (HM) techniques, which manipulate an acquired histogram before the equalization, have been introduced. Wang and Ward [11] clamped large histogram values and then modified the resulting histogram using the power law. Lee *et al.* [12] employed a logarithm function to reduce large histogram values effectively, preventing the transformation function from having too steep slopes. Several researches also have been carried out to extend the conventional HE to the multidimensional histograms of color images. Naik and Murthy [13] generalized HE to enhance the contrast of color images and developed an algorithm to avoid the gamut problem during the enhancement. Han *et al.* [14] proposed the iso-luminance HE algorithm for enhancing RGB images, which achieves the uniform histogram of the luminance channel.

These global CE techniques [7]–[14] process the histograms of input images to obtain output images. The histogram processing has the advantages of straightforward implementation and computational efficiency, since it achieves significant data reduction. However, it discards the spatial information in the unordered summarization process [15]. In other words, the histogram cannot capture the joint relationships between neighboring pixels. Recently, a few CE algorithms have been developed to consider spatial image features by extending the notion of the histogram. Arici *et al.* [16] constructed the histogram of an input image adaptively to image char-

This work was supported partly by the National Research Foundation of Korea (NRF) grant funded by the Ministry of Science, ICT & Future Planning (MSIP) (No. 2009-0083495), and partly by the NRF grant funded by the Korea government (MSIP) (No. 2012-011031).

Preliminary results of this work were published in Proc. IEEE ICIP, 2012 [1].

C. Lee and C.-S. Kim are with the School of Electrical Engineering, Korea University, Seoul 136-713, Korea. E-mails: {wiserain, changsukim}@korea.ac.kr.

C. Lee was with the School of Electrical Engineering, Korea University, Seoul 136-713, Korea. He is now with the Department of Electrical Engineering, The Pennsylvania State University, University Park, PA 16802, USA. E-mail: cxl59@psu.edu.

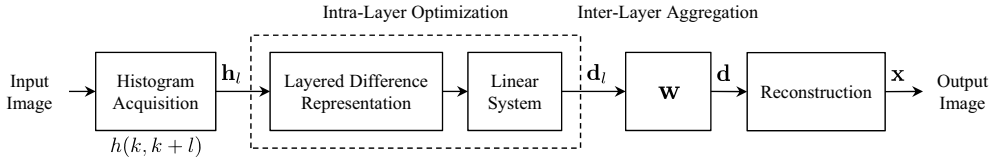

Fig. 1. An overview of the proposed algorithm.

acteristics. They reduced large histogram values for smooth areas corresponding to background regions to focus on the enhancement of foreground objects. However, their algorithm does not use the joint relationships between pixels explicitly for the enhancement. Celik and Tjahjadi [17] constructed a 2D histogram, which recorded the numbers of gray-level pairs in an input image, and modified it to emphasize large gray-level differences. Then, they achieved CE by mapping the diagonal elements of the 2D input histogram to those of the 2D modified histogram. However, their mapping scheme may not handle large histogram values appropriately and may yield over-stretching artifacts.

In this work, we propose a novel global CE algorithm based on the layered difference representation (LDR). The proposed algorithm also uses a 2D histogram, but adopts a different theoretical approach. We first obtain the 2D histogram of gray-level differences between neighboring pixels. We attempt to amplify gray-level differences, occurring frequently in the input image, to enhance the contrast. To this end, we represent output gray-level differences and the transformation function in a tree-like layered structure. This representation is called the LDR. Then, at each layer, we formulate a constrained optimization problem for the enhancement and solve it efficiently to obtain the difference vector. Finally, we aggregate the difference vectors at all layers into a single unified difference vector, which is equivalent to the transformation function. Extensive experimental results demonstrate that the proposed algorithm yields higher image qualities than the conventional HE [7], the Arici *et al.*'s algorithm [16], and the Celik and Tjahjadi's algorithm [17].

The rest of this paper is organized as follows. Section II describes the proposed algorithm, and Section III addresses implementation details. Section IV discusses experimental results. Finally, Section V concludes the paper.

II. Proposed Algorithm

We propose a CE algorithm based on the LDR. As shown in Fig. 1, the proposed algorithm has two main components: intra-layer optimization and inter-layer aggregation. We first extract a 2D histogram $h(k, k+l)$ from an input image, by counting the pairs of adjacent pixels with gray-levels k and $k+l$. In the intra-layer optimization, we obtain the histogram vector $\mathbf{h}_l$ at each layer l and use it to formulate a system of linear equations. By solving the system, we obtain the difference vector $\mathbf{d}_l$ at layer l. Next, in the inter-layer aggregation, we combine the difference vectors at all layers into the unified difference vector $\mathbf{d}$ using the weighting vector $\mathbf{w}$. We then reconstruct the transformation function $\mathbf{x}$ from $\mathbf{d}$ and transform the input image to the output image.

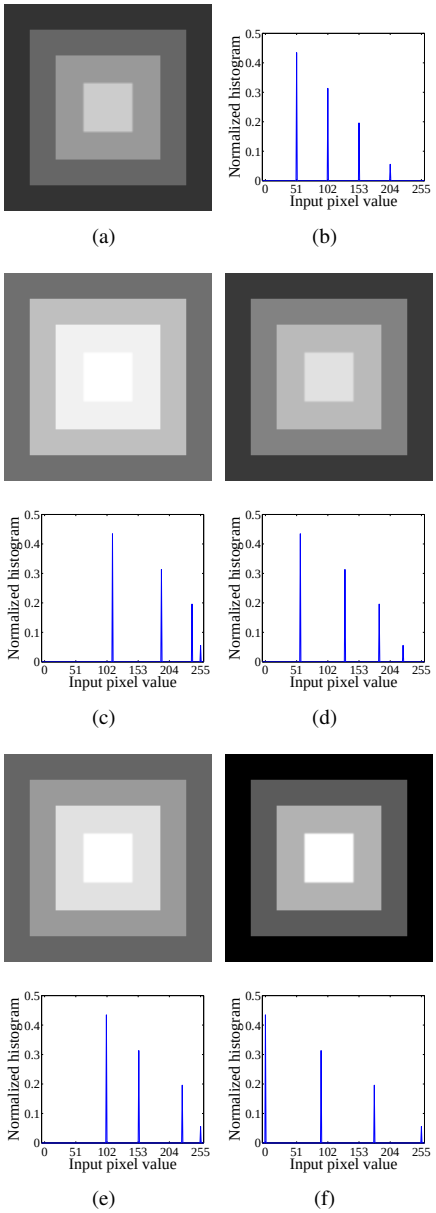

Fig. 2. Comparative tests of the conventional algorithms and the proposed algorithm on a synthetic input image: (a) the input image, (b) its normalized histogram, and (c)∼(f) the output images and their normalized histograms, obtained by HE [7], WAHE [16], CVC [17] and the proposed algorithm, respectively.

A. Motivation

Since the human visual system (HVS) is more sensitive to gray-level differences between neighboring pixels than to absolute gray-levels [18], [19], we can achieve perceptual CE by emphasizing the differences. However, most enhancement

algorithms [4]–[14] focus on the first-order distribution of absolute gray-levels in an image, without considering the spatial placement of those gray-levels nor the joint gray-level distribution of neighboring pixels. Therefore, these conventional algorithms may fail to provide visually satisfying images.

To clarify differences between the conventional algorithms and the proposed algorithm, we perform tests on a synthetic image in Fig. 2(a), which has four overlapping squares with different gray-levels. As shown in the normalized histogram in Fig. 2(b), the image does not exploit the full dynamic range and its gray-levels are confined to the range of $[51, 204]$. To enhance the contrast, the gray-level distribution should be stretched to the full dynamic range: the lowest and the highest gray-levels in the input histogram should be mapped to the minimum and the maximum gray-levels, respectively. However, this cannot be achieved by the conventional algorithms. HE [7] causes a steep slope in the transformation function, when a histogram bin has a large value. In this example, the lowest gray-level, 51, composes more than 40% of the input image. HE hence makes the lowest gray-level even brighter, degrading the quality of the output image in Fig. 2(c). WAHE [16] in Fig. 2(d) alleviates the over-enhancement problem in HE and maintains a similar dynamic range to the input image. But, it fails to achieve further enhancement. To the best of our knowledge, CVC [17] was the first CE algorithm, which adopted a 2D histogram to use the contextual information in an image, such as edges and object boundaries. However, it does not fully exploit the relationship between input gray-level differences and output gray-level differences. Therefore, CVC reduces the contrast in Fig. 2(e).

On the contrary, the proposed algorithm considers the statistics of gray-level differences, instead of absolute gray-levels, and derives a desirable relationship between the 2D histogram of the input image and the gray-level differences in the output image. Consequently, the gray-level differences, which occur frequently across the square boundaries in the input image, are amplified in the output image to improve the contrast. Fig. 2(f) shows that the proposed algorithm exploits the full dynamic range and outputs a higher contrast image than the conventional algorithms.

Let us describe the proposed algorithm in detail subsequently.

B. Layered Difference Representation

For the sake of notational simplicity, let us consider a typical 8-bit imaging system, in which the maximum gray-level is 255. Let $\mathbf{x} = [x_0, x_1, \cdots, x_{255}]^T$ denote the transformation function, which maps gray-level k in the input image to gray-level x_k in the output image [12]. To derive a desirable transformation function, we introduce the LDR. Suppose that a pair of adjacent pixels in the input image have gray-levels k and $k+l$. Then, they are mapped to gray-levels x_k and x_{k+l} in the output image, respectively. The difference variable d_k^l at layer l is then defined as

$$d_k^l = x_{k+l} - x_k \quad \text{for } 0 \le k \le 255 - l. \tag{1}$$

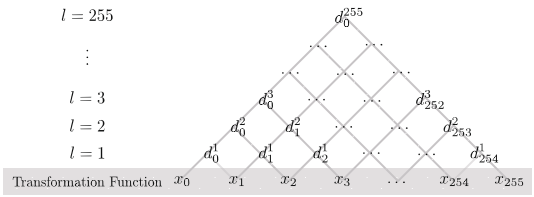

Fig. 3. The layered difference representation (LDR): the transformation function $\mathbf{x} = [x_0, x_1, \cdots, x_{255}]^T$ and the difference variables d_k^l's are shown in a tree-like pyramidal structure.

Notice that the input gray-level difference l between k and $k+l$ is mapped to the output gray-level difference d_k^l.

Let the 2D histogram $h(k, k+l)$ represent the number of pairs of adjacent pixels with values k and $k+l$ in the input image. Different types of neighborhood can be employed, but the simple 4-adjacency is used in this work. In many histogram-based CE algorithms [8], [10], [11], [16], [17], [20], the transformation function gets an extreme slope when a histogram bin has a very large value. As a result, output images are often degraded by the contrast over-stretching. Peak values in the 2D histogram can cause similar over-enhancement. To reduce such peaks and relax steep slopes, we modify the 2D histogram using a logarithm function, which is monotonically increasing and can decrease large values effectively. Note that Lee *et al*. [12] also used a logarithm function to attenuate the 1-D histogram of an input image. Also, the order of adjacent pixels is not important. Therefore, we obtain an unordered logarithm-attenuated 2D histogram

$$h_k^l = \log\left(h(k, k+l) + h(k+l, k)\right), \quad 0 \le k \le 255 - l. \tag{2}$$

A large h_k^l indicates that the gray-level pairs $(k, k+l)$ or $(k+l, k)$ appear frequently in the input. In such a case, the difference variable d_k^l should be large, so that those frequent pairs have a large gray-level difference in the output. In other words, d_k^l should be proportional to h_k^l to improve the output contrast. Therefore, at each layer, we have the desirable relationship

$$d_k^l = \kappa_l \times h_k^l, \quad 0 \le k \le 255 - l, \tag{3}$$

where κ_l is a normalizing constant at layer l.

Our objective is to design the transformation function $\mathbf{x}$ that satisfies the system of equations in (1) and (3). However, this system does not have an exact solution. We develop an algorithm to provide an approximate solution instead. Before describing the algorithm, let us state two elementary properties of the system of equations. Fig. 3 shows the LDR, which depicts the transformation function $\mathbf{x}$ and the difference variables d_k^l's in a tree-like pyramidal structure[1].

First, the transformation function $\mathbf{x}$ can be completely determined by the difference variables d_k^1's at layer 1. Specifically,

$$x_k = \sum_{i=0}^{k-1} d_i^1 \quad \text{for } 1 \le k \le 255, \tag{4}$$

[1]Precisely speaking, it is not a tree, since two parents cannot have a common child in a tree [21].

and $x_0 = 0$ since the darkest level in the input should be mapped to the darkest level in the output to preserve the dynamic range. Therefore, we can solve the system of equations in terms of d_k^1's and then reconstruct the transformation function using (4).

Second, the difference variables d_k^l's at higher layers also can be expressed by those d_k^1's at layer 1. From (1), we have

$$d_k^l = \sum_{i=k}^{k+l-1} d_i^1, \quad 0 \le k \le 255 - l. \tag{5}$$

In the LDR in Fig. 3, each difference variable d_k^l at layer l is equal to the sum of its descendants at layer 1. For instance, from (1) and (4), the first element of difference variables at layer 3 can be rewritten as

$$\begin{aligned} d_0^3 &= x_3 - x_0 = x_3 - x_2 + x_2 - x_1 + x_1 - x_0 \\ &= d_2^1 + d_1^1 + d_0^1. \end{aligned} \tag{6}$$

Thus, the difference variables d_k^l's have a strong structure across layers. On the other hand, the 2D histogram values h_k^l's do not have such a strong structure. Therefore, we cannot satisfy the proportional relationships in (3) exactly and should obtain an approximate solution instead.

C. Intra-Layer Optimization

Given the 2D histogram h_k^l of the input image in (2), we should decide the difference variables d_k^1's at layer 1, which satisfy the equations in (3) and (5). More specifically, by considering the relationships in (3) at all layers and expressing d_k^l's in terms of the variables d_k^1's via (5), we can construct a system of linear equations. The system is over-determined, since there are more observations h_k^l's than the variables d_k^1's. Also, each d_k^1 should be nonnegative to ensure a monotonically increasing transformation function $\mathbf{x}$ [12]. We can solve this over-determined system with the nonnegative constraint based on the nonnegative least squares (NNLS) technique [22]. However, as mentioned before, d_k^l's have a strong structure across layers. NNLS, which considers all layers in a single system, hence yields an undesirable solution. Moreover, NNLS is sensitive to magnitude variations in the 2D histogram. For example, Fig. 4(a) shows the histogram h_k^l for an input image in Fig. 4(d). Histogram components around h_{35}^1 and h_{139}^1 are much larger than the others. In the least squares optimization, the sum of the squared errors is dominated by these large components. As a result, the other histogram components contribute little to the solution, and the difference variables in Fig. 4(b) are irregular and noisy. Therefore, the transformation function in Fig. 4(c) is not smooth and causes contour artifacts in the output image in Fig. 4(e).

The example in Fig. 4 indicates that it is necessary to process the information at each layer separately, instead of considering all layers in a single system. In other words, we ignore the inter-layer dependencies temporarily and solve the system of equations at each layer separately. More specifically, for each layer index l, we obtain and solve the reduced system of equations in (3) and (5). We then aggregate the separate solutions for different layers to form the overall solution, as

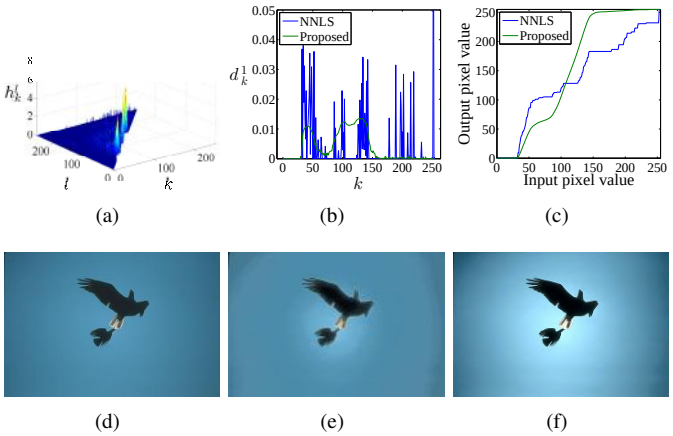

Fig. 4. The enhancement of the "Eagle" image. For better evaluation of image qualities, we recommend the readers to see this figure on display devices rather than the printed version. (a) 2D histogram. (b) Difference vector. (c) Transformation function. (d) Input. (e) NNLS. (f) Proposed.

will be described in Section II-E. Fig. 4(f) shows that the proposed algorithm provides a higher quality image with less contour artifacts than the NNLS technique.

At each layer l, d_k^l's are determined by the 2D histogram values h_k^l's via (3). Also, each d_k^l is the sum of d_k^1's in (5). Therefore, we can form a linear equation

$$\mathbf{A}_l \mathbf{d}_l = \kappa_l \mathbf{h}_l, \tag{7}$$

where $\mathbf{A}_l \in \mathbb{R}^{(256-l)\times 255}$ is a binary matrix composed of 0 and 1, $\mathbf{d}_l = [d_0^1, d_1^1, \cdots, d_{254}^1]^T$ is the difference vector to be determined, and $\mathbf{h}_l = \left[h_0^l, h_1^l, \cdots, h_{255-l}^l\right]^T$ is the column vector representing the observed 2D histogram values at layer l. For instance, at layer 2, the linear equation $\mathbf{A}_2\mathbf{d}_2 = \kappa_2\mathbf{h}_2$ is given by

$$\begin{bmatrix} 1 & 1 & 0 & \cdots & 0 & 0 & 0 \\ 0 & 1 & 1 & \cdots & 0 & 0 & 0 \\ 0 & 0 & 1 & \cdots & 0 & 0 & 0 \\ \vdots & \vdots & \vdots & \ddots & \vdots & \vdots & \vdots \\ 0 & 0 & 0 & \cdots & 1 & 1 & 0 \\ 0 & 0 & 0 & \cdots & 0 & 1 & 1 \end{bmatrix} \begin{bmatrix} d_0^1 \\ d_1^1 \\ d_2^1 \\ \vdots \\ d_{253}^1 \\ d_{254}^1 \end{bmatrix} = \kappa_2 \begin{bmatrix} h_0^2 \\ h_1^2 \\ h_2^2 \\ \vdots \\ h_{252}^2 \\ h_{253}^2 \end{bmatrix}. \tag{8}$$

In this way, at each layer l, we obtain the difference vector $\mathbf{d}_l$ by solving the constrained optimization problem:

$$\text{minimize} \quad \|\mathbf{A}_l\mathbf{d}_l - \kappa_l\mathbf{h}_l\|^2 \tag{9}$$

$$\text{subject to} \quad \mathbf{d}_l \succeq \mathbf{0}, \tag{10}$$

$$\mathbf{1}^T\mathbf{d}_l = 255, \tag{11}$$

where $\mathbf{1}$ and $\mathbf{0}$ denote the column vectors, all elements of which are 1 and 0, respectively. Also, $\mathbf{a} \succeq \mathbf{0}$ means that all elements in vector $\mathbf{a}$ are greater than or equal to 0. The inequality in (10) and the equality in (11) are the constraints to guarantee that the transformation function is monotonically increasing and preserves the dynamic range $x_{255} = 255$, respectively [12].

Since (9) is a quadratic cost function of $\mathbf{d}_l$, various techniques [23] can be employed to solve the optimization problem in general. However, as the layer index l increases, the number

of observations gets much less than the number of unknown variables, so that the problem becomes ill-conditioned except for the layer $l = 1$. Note that reasonable solutions can be found assuming the sparsity of the solutions [24]. However, finding the sparsest solutions is NP-hard [25], and the solution $\mathbf{d}_l$ to our problem cannot be sparse due to the constraints in (10) and (11). Thus, instead of employing the sparse coding techniques, we solve the intra-layer optimization problem by incorporating additional equalities, which convert the original problem into an over-determined one. Then, we obtain the solution to the over-determined problem efficiently using the method of least squares. Let us detail the solution in the subsequent section.

D. Solution to the Optimization Problem

The constrained optimization problem in (9)∼(11) cannot be solved directly in its original form. However, fortunately, assuming that the descendants of each d_k^l are equal to one another, we can obtain the solution vector $\mathbf{d}_l$ at each layer l.

Let us recall that, in the LDR, each difference variable d_k^l can be expressed as the sum of its descendants at layer 1 in (5). In addition to this relation, we assume that those descendants have the same value. More specifically, given a difference variable d_k^l, $l > 1$, we assume that its descendants at layer 1 satisfy

$$d_i^1 = d_j^1 \quad \text{for } k \le i, j \le k + l - 1. \tag{12}$$

This implies that the output transformation function should increase linearly between x_k and x_{k+l}. By incorporating these additional equalities in (12) into the optimization problem in (9)∼(11), we can convert it into an over-determined system and solve it using the method of least squares. Incorporating these equalities is reasonable, since the transformation function should be smooth to avoid artifacts in the output image. Furthermore, in Section III, we will show that the smoothness assumption also enables a computationally efficient solution.

From (3) and (5), the smoothness assumption can be written as l equations, given by

$$d_k^1 = \cdots = d_{k+l-1}^1 = \frac{\kappa_l}{l} h_k^l. \tag{13}$$

Similarly, the linear equation in (7) can be decomposed into l equations,

$$\mathbf{A}_{l,1}\mathbf{d}_l = \cdots = \mathbf{A}_{l,l}\mathbf{d}_l = \frac{\kappa_l}{l}\mathbf{h}_l, \tag{14}$$

where $\mathbf{A}_{l,i}$ is a binary matrix of the same size as $\mathbf{A}_l$ in (7). The $(j, i + j)$th elements of $\mathbf{A}_{l,i}$ are 1 and the others are 0. For example, $\mathbf{A}_2$ in (8) is decomposed into two matrices as

$$\mathbf{A}_{2,1} = \begin{bmatrix} 1 & 0 & 0 & \cdots & 0 & 0 & 0 \\ 0 & 1 & 0 & \cdots & 0 & 0 & 0 \\ 0 & 0 & 1 & \cdots & 0 & 0 & 0 \\ \vdots & \vdots & \vdots & \ddots & \vdots & \vdots & \vdots \\ 0 & 0 & 0 & \cdots & 1 & 0 & 0 \\ 0 & 0 & 0 & \cdots & 0 & 1 & 0 \end{bmatrix} \text{ and}$$

$$\mathbf{A}_{2,2} = \begin{bmatrix} 0 & 1 & 0 & \cdots & 0 & 0 & 0 \\ 0 & 0 & 1 & \cdots & 0 & 0 & 0 \\ 0 & 0 & 0 & \cdots & 0 & 0 & 0 \\ \vdots & \vdots & \vdots & \ddots & \vdots & \vdots & \vdots \\ 0 & 0 & 0 & \cdots & 0 & 1 & 0 \\ 0 & 0 & 0 & \cdots & 0 & 0 & 1 \end{bmatrix}. \tag{15}$$

Since the difference vector $\mathbf{d}_l$ should satisfy l linear equations in (14) simultaneously, we can rewrite the linear equation in (7) as

$$\mathbf{B}_l\mathbf{d}_l = \phi_l\mathbf{g}_l, \tag{16}$$

where $\phi_l = \frac{\kappa_l}{l}$ and

$$\mathbf{B}_l = \begin{bmatrix} \mathbf{A}_{l,1} \\ \vdots \\ \mathbf{A}_{l,l} \end{bmatrix} \text{ and } \mathbf{g}_l = \begin{bmatrix} \mathbf{h}_l \\ \vdots \\ \mathbf{h}_l \end{bmatrix}. \tag{17}$$

We converted the under-determined system in (7) into the over-determined system in (16). Therefore, the optimization problem in (9)∼(11) becomes the problem of determining the difference vector $\mathbf{d}_l$, which minimizes the squared distance $\|\mathbf{B}_l\mathbf{d}_l - \phi_l\mathbf{g}_l\|^2$ subject to the constraints in (10) and (11). We solve this constrained optimization problem by minimizing the Lagrangian cost function

$$J(\mathbf{d}_l) = \|\mathbf{B}_l\mathbf{d}_l - \phi_l\mathbf{g}_l\|^2 + \lambda_l\left(\mathbf{1}^T\mathbf{d}_l - 255\right), \tag{18}$$

where λ_l is a Lagrangian multiplier. By differentiating (18) with respect to $\mathbf{d}_l$ and setting it to zero, we obtain the optimal difference vector

$$\mathbf{d}_l = \phi_l\left(\mathbf{B}_l^T\mathbf{B}_l\right)^{-1}\left(\mathbf{B}_l^T\mathbf{g}_l - \mu_l\mathbf{1}\right), \tag{19}$$

where the constant μ_l, satisfying the constraint in (11), is given by

$$\mu_l = \frac{\phi_l\mathbf{1}^T\left(\mathbf{B}_l^T\mathbf{B}_l\right)^{-1}\mathbf{B}_l^T\mathbf{g}_l - 255}{\phi_l\mathbf{1}^T\left(\mathbf{B}_l{}^T\mathbf{B}_l\right)^{-1}\mathbf{1}}. \tag{20}$$

Whereas the equality constraint in (11) is satisfied by (20), the non-negative constraint in (10) still depends on the choice of the normalizing constant ϕ_l. As will be shown in Section III, all elements in both $\left(\mathbf{B}_l^T\mathbf{B}_l\right)^{-1}$ and $\mathbf{B}_l^T\mathbf{g}_l$ in (19) are non-negative. Therefore, notice from (19) that the non-negative constraint is satisfied when $\min(\mathbf{B}_l^T\mathbf{g}_l) \ge \mu_l$. Then, from (20), we derive the possible range for ϕ_l, which is given by

$$0 < \phi_l \le \phi_l^{\max} = \frac{255}{\mathbf{1}^T\left(\mathbf{B}_l^T\mathbf{B}_l\right)^{-1}\mathbf{B}_l^T\mathbf{g}_l - \min(\mathbf{B}_l^T\mathbf{g}_l)\cdot\mathbf{1}^T\left(\mathbf{B}_l{}^T\mathbf{B}_l\right)^{-1}\mathbf{1}}. \tag{21}$$

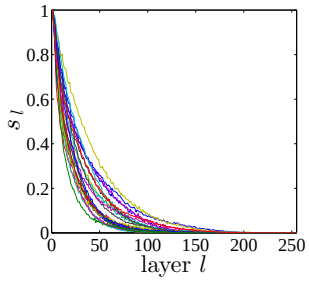

Fig. 5. Normalized distributions of s_l's for various test images.

We have experimentally found that a larger ϕ_l provides higher contrast. We hence fix the normalizing constant $\phi_l = \phi_l^{\max}$, or equivalently $\mu_l = \min(\mathbf{B}_l^T \mathbf{g}_l)$. Then, the optimal difference vector $\mathbf{d}_l$ is given by

$$\mathbf{d}_l = \phi_l^{\max} \left(\mathbf{B}_l^T \mathbf{B}_l\right)^{-1} \left(\mathbf{B}_l^T \mathbf{g}_l - \min(\mathbf{B}_l^T \mathbf{g}_l) \cdot \mathbf{1}\right). \quad (22)$$

Notice that $\mathbf{B}_l$ is a sparse binary matrix, and $\mathbf{g}_l$ is constructed by repeating the histogram vector $\mathbf{h}_l$. Therefore, the number of operations for the matrix multiplication and the matrix inversion can be reduced significantly, despite of the large dimensions. We will describe the efficient implementation method in Section III.

E. Inter-Layer Aggregation

By performing the intra-layer optimization at each layer, we obtain 255 difference vectors $\mathbf{d}_l$'s, $1 \le l \le 255$. We aggregate these difference vectors to form a unified difference vector $\mathbf{d}$.

We obtain $\mathbf{d}_l$ from the histogram $\mathbf{h}_l = \left[h_0^l, h_1^l, \cdots, h_{255-l}^l\right]^T$ of pixel pairs, whose gray-level differences are l, based on the relationship in (3). For a typical input image, most elements in $\mathbf{h}_l$ are zero when l is large. In other words, $\mathbf{h}_l$ becomes sparser as l gets larger. Inspired by this observation, we assume that the reliability of $\mathbf{d}_l$ is proportional to $s_l = \sum_k h_k^l$, which is the total number of pixel pairs with the gray-level difference l. Fig. 5 shows s_l's for various test images, which are normalized by the maximum values. We see that, as l increases, the occurrence frequency s_l gets lower. We adjust the relative contribution of $\mathbf{d}_l$ based on its reliability s_l. Therefore, $\mathbf{d}_l$ at a higher layer l has a less impact on the unified difference vector $\mathbf{d}$.

We first normalize s_l's to w_l's by dividing it with the maximum value and applying a simple power law function with a user-controllable parameter α. Specifically, we obtain the weighting vector $\mathbf{w} = [w_1, w_2, \cdots, w_{255}]^T$, whose lth element is given by

$$w_l = \left(\frac{s_l}{\max_i s_i}\right)^{\alpha}. \quad (23)$$

Then, we obtain the unified difference vector $\mathbf{d}$ by

$$\mathbf{d} = \frac{1}{\mathbf{1}^T \mathbf{w}} \mathbf{D}\mathbf{w}, \quad (24)$$

where $\mathbf{D} \in \mathbb{R}^{255 \times 255}$ is a concatenated matrix whose ith column is $\mathbf{d}_i$. Finally, we obtain the transformation function $\mathbf{x}$ from the unified difference vector $\mathbf{d}$ via

$$x_k = \sum_{i=0}^{k-1} d_i \quad \text{for } 1 \le k \le 255, \quad (25)$$

and $x_0 = 0$.

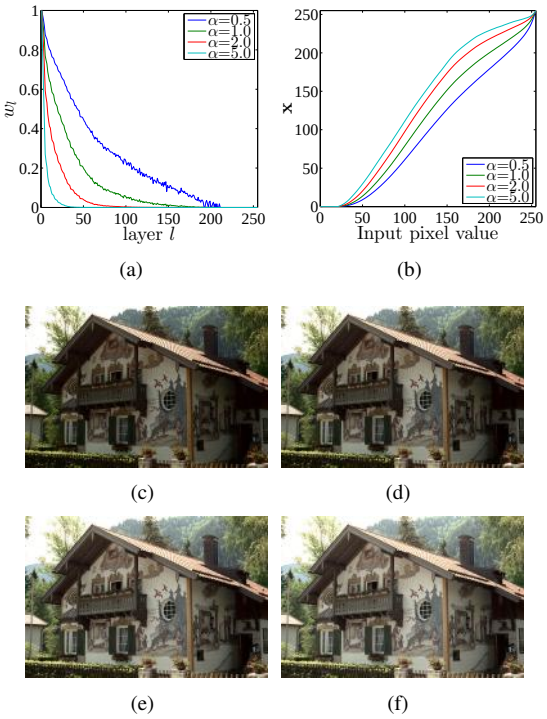

Fig. 6. Impacts of the parameter α on output images: (a) weights w_l's, (b) the transformation functions, and (c)∼(f) the corresponding output images at α=0.5, 1.0, 2.0, and 5.0, respectively.

Fig. 6 illustrates the impacts of the parameter α. Fig. 6(a) and (b) show w_l's and the transformation functions for an input image, when $\alpha = 0.5, 1.0, 2.0$, or 5.0, respectively. Fig. 6(c)∼(f) are the corresponding output images. As α gets smaller, $\mathbf{d}_l$'s at high layers are superposed with bigger weights to form the unified difference vector $\mathbf{d}$. This causes the output images in Fig. 6(c) and (d) to lose details in dark regions. On the other hand, by increasing α, we can enhance the image qualities and provide fine details in Fig. 6(e) and (f). We have experimentally found that $\alpha > 1.5$ provides satisfactory results, by weighting reliable vectors at low layers more heavily in the aggregation process. Notice that α is the only parameter in the proposed algorithm.

III. Implementation

The direct matrix computation of $\mathbf{d}_l$ in (22) demands high computation complexity due to the huge dimensions of $\mathbf{B}_l$ and $\mathbf{g}_l$. However, as defined in (17), these matrices are constructed by concatenating simple sub-matrices vertically. Thus, we can rewrite $\mathbf{B}_l^T \mathbf{B}_l$ and $\mathbf{B}_l^T \mathbf{g}_l$ in (22) as

$$\mathbf{B}_l^T \mathbf{B}_l = \sum_{i=1}^{l} \mathbf{A}_{l,i}^T \mathbf{A}_{l,i}, \quad (26)$$

$$\mathbf{B}_l^T \mathbf{g}_l = \sum_{i=1}^{l} \mathbf{A}_{l,i}^T \mathbf{h}_l = \mathbf{A}_l^T \mathbf{h}_l, \quad (27)$$

respectively.

Let us analyze each matrix multiplication to obtain a simplified form. First, $\mathbf{A}_{l,i} \in \mathbb{R}^{(256-l)\times 255}$ is a rectangular matrix, in which ith to $(i+255-l)$th columns constitute an identity matrix $\mathbf{I}_l \in \mathbb{R}^{(256-l)\times(256-l)}$ and all the others are zero columns. For instance, $\mathbf{A}_{5,2} = [\mathbf{0}, \mathbf{I}_5, \mathbf{0}, \mathbf{0}, \mathbf{0}]$. Therefore, $\mathbf{A}_{l,i}^T \mathbf{A}_{l,i}$ is a diagonal matrix, in which ith to $(i+255-l)$th diagonal elements are 1 and the others are 0. The sum $\mathbf{B}_l^T \mathbf{B}_l = \sum_{i=1}^{l} \mathbf{A}_{l,i}^T \mathbf{A}_{l,i}$ in (26) is also a diagonal matrix $\mathbf{U}_l$, in which the kth diagonal element u_k^l is given by

$$u_k^l = \min(k, 256-l) - \max(k-l, 0) \quad \text{for } 1 \le k \le 255. \tag{28}$$

In the case of $l = 5$, we have $\mathbf{U}_5 = \text{diag}\big([1, 2, 3, 4, 5, 5, \cdots, 5, 5, 4, 3, 2, 1]\big)$.

Second, the matrix multiplication $\mathbf{A}_l^T \mathbf{h}_l$ in (27) involves the summation of l successive elements in $\mathbf{h}_l$. Let $\mathbf{m}_l = \mathbf{A}_l^T \mathbf{h}_l$ denote the resulting column vector. Then, its kth element m_k^l is given by

$$m_k^l = \sum_{i=\max(k-l,0)}^{\min(k-1,255-l)} h_i^l \quad \text{for } 1 \le k \le 255. \tag{29}$$

This summation can be interpreted as the convolution

$$\mathbf{m}_l = \mathbf{h}_l * \mathbf{1}_l, \tag{30}$$

where $\mathbf{1}_l$ is the column vector of length l, whose elements are all 1. Also, $*$ denotes the convolution operator.

Consequently, the original matrix multiplications in (26) and (27) are simplified to

$$\mathbf{B}_l^T \mathbf{B}_l = \mathbf{U}_l, \tag{31}$$

$$\mathbf{B}_l^T \mathbf{g}_l = \mathbf{m}_l, \tag{32}$$

respectively. Finally, we have the compact representation of (22), given by

$$\mathbf{d}_l = \phi_l^{\max} \mathbf{U}_l^{-1} \left(\mathbf{m}_l - \min(\mathbf{m}_l) \cdot \mathbf{1} \right). \tag{33}$$

The inverse matrix $\mathbf{U}_l^{-1}$ is also diagonal, and its kth diagonal element is $1/u_k^l$. Therefore, the computational complexity to calculate $\mathbf{d}_l$ is reduced from $\mathcal{O}(K^3)$ in (22) to $\mathcal{O}(K)$ in (33), where K denotes the total number of gray-levels. Furthermore, we can accelerate the processing further by computing $\mathbf{U}_l^{-1}$ in advance.

IV. Experimental Results

We select test images of resolution 768×512 from the Kodak Lossless True Color Image Suite [26], test images of resolution 512×512 from the USC-SIPI Database [27], test images of resolution 481×312 from the Berkeley Image Data Set [28], and test images captured from commercial digital cameras. In total, we use 600 test images. We compare the proposed algorithm with the conventional HE [7], WAHE [16] and CVC [17] algorithms. For WAHE, the parameter g is fixed to 1.5 to yield the best overall image quality. For CVC, the parameters are set to $\alpha = \beta = \gamma = \frac{1}{3}$ and the 7×7 neighborhood is used, as suggested in [17]. In the proposed algorithm, the only controllable parameter is α in (23). We fix α to 2.5 in all experiments to provide the best overall performance in terms of the objective quality metrics, which will be explained in Section IV-A. We process luminance components only in the experiments. Specifically, given a color image, we convert it to the YUV color space, and then process only the Y component without modifying the U and V components.

TABLE I

Objective quality assessment of CE algorithms using four metrics: discrete entropy (DE) [29], measure of enhancement (EME) [30], absolute mean brightness error (AMBE) [10], and PixDist [31]. For each metric, the best and the second best results are boldfaced and underlined, respectively.

	Input	HE	WAHE	CVC	Proposed
DE	7.11	6.91	<u>7.05</u>	7.04	**7.07**
EME	18.89	**31.65**	19.04	29.33	<u>30.32</u>
AMBE	-	30.04	**10.23**	<u>12.28</u>	13.13
PixDist	28.08	**42.21**	33.93	34.75	<u>36.70</u>

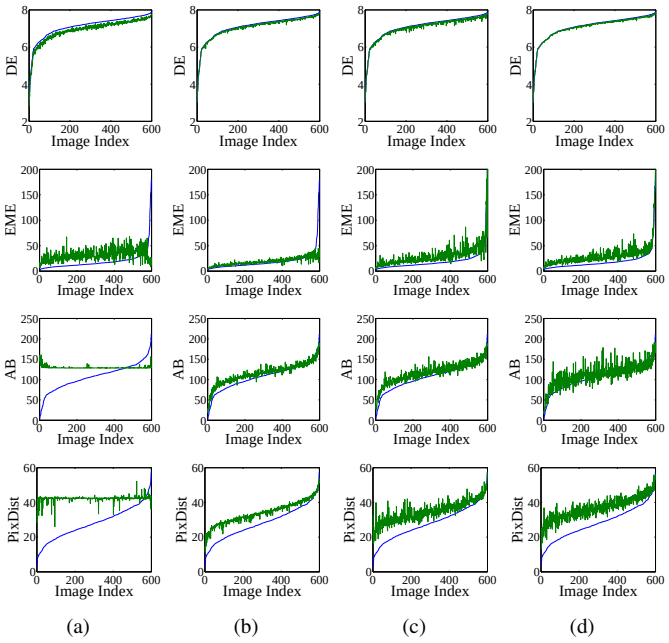

Fig. 7. Objective metric scores on 600 test images. From top to bottom, the four rows plot the DE, EME, average brightness (AB), and PixDist scores. The measurements from the input images are plotted in blue, whereas those from the enhanced images are displayed in green. (a) HE. (b) WAHE. (c) CVC. (d) Proposed.

A. Objective Assessment

We assess the CE performance objectively using four quality metrics: discrete entropy (DE) [29], measure of enhancement (EME) [30], absolute mean brightness error (AMBE) [10], and PixDist [31]. Table I lists the average performance on the 600 test images. For each metric, the best and the second best results are boldfaced and underlined, respectively.

First, DE measures the amount of information in an image: a high DE indicates that the image contains more variations and conveys more information. Because of the information processing inequality [32], no output image, processed by any transformation function, can have a higher DE than the input image. Thus, the proposed algorithm provides a lower average

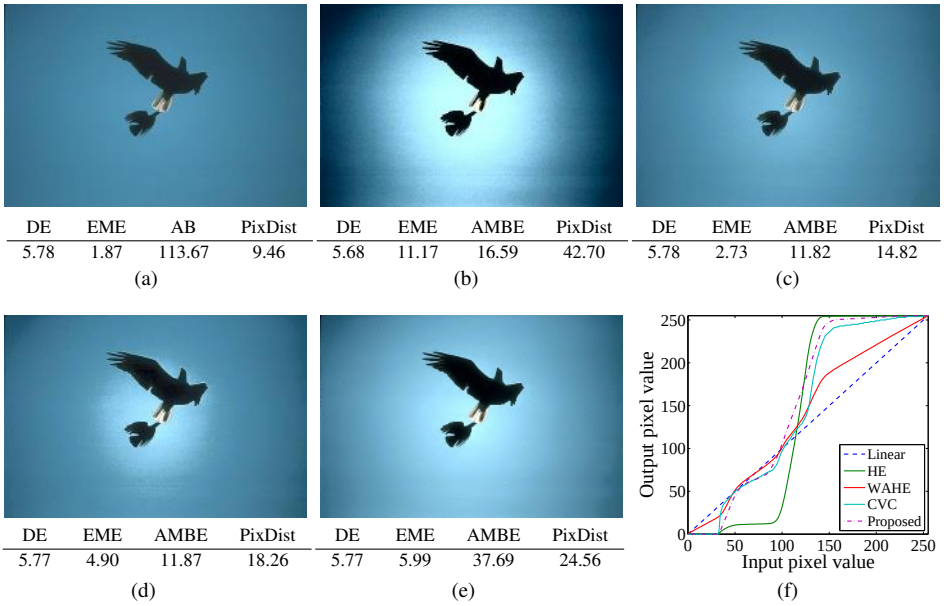

Fig. 8. CE results on the "Eagle" image: (a) input image, (b) HE, (c) WAHE, (d) CVC, (e) the proposed algorithm, and (f) the comparison of the corresponding transformation functions.

DE than the input. But, the proposed algorithm conveys more information than all the conventional algorithms.

Second, EME approximates the average contrast in an image by dividing the image into blocks, computing a score based on the minimum and the maximum gray-levels in each block, and averaging the scores. The block size is set to 8×8 in this experiment. HE provides the best EME score, but it causes over-stretching or over-enhancement artifacts, as will be illustrated in the next section. Since CVC and the proposed algorithm exploit the 2D contextual information and enhance local details efficiently, they yield significantly better EME scores than WAHE.

Third, AMBE measures the absolute difference between input and output gray-level means. A lower value implies that the corresponding algorithm well preserves the mean brightness of an input image. WAHE incurs the lowest brightness change, since it reduces the abnormality by averaging its transformation function with the linear transformation function. The proposed algorithm ranks third. However, WAHE, CVC, and the proposed algorithm provide similar AMBE scores, which are significantly better than the score of HE.

Fourth, PixDist computes the average gray-level difference over all pixel pairs in an image. It yields a high score when histogram components are uniformly distributed without concentrating at particular gray-levels. Except for the contrast over-stretching HE algorithm, the proposed algorithm provides the best performance in terms of PixDist.

To evaluate the performance variations on individual test images, we plot the metric scores of output images in comparison with those of input images in Fig. 7. In each graph, the 600 input images are indexed so that their scores are sorted in the ascending order. For DE, the proposed algorithm provides the best performance, which is very close to the input curve. For EME, the proposed algorithm enhances the score of every input image. In contrast, the conventional algorithms reduce the scores of some input images, especially when the input scores are high. In the case of AMBE, the average brightness (AB) is plotted instead of the brightness error. The proposed algorithm causes bigger variations in AB than the conventional algorithms, since it is more adaptive to local image details and structures. For PixDist, the proposed algorithm increases the score of every input image.

B. Subjective Assessment

Even though an image provides a higher objective quality score than another image, its subjective visual quality is not always superior accordingly. In this section, we provide examples of output images to assess their qualities subjectively and analyze the characteristics of the proposed algorithm in comparison with those of the conventional algorithms.

Fig. 8 shows the CE results on the "Eagle" image, which is mainly composed of a sky region with similar gray-levels in the range of $[100, 140]$. This region causes a high peak in the input histogram, which HE and CVC cannot handle properly. More specifically, HE and CVC yield steep slopes in their transformation functions, when the input gray-level is between 100 and 140, as shown in Fig. 8(f). Thus, HE and CVC increase the contrast on the smooth region excessively, producing contour artifacts. Both WAHE and the proposed algorithm effectively reduce the histogram peak and suppress the contour artifacts. Furthermore, compared with WAHE, the proposed algorithm provides a more distinctive silhouettes of the eagles and better local contrast on the eagle's tail. In this example, the minimum input gray-level is 23. WAHE expresses the darkest pixels less darker than the other algorithms by starting its output gray-level from 14. Therefore, WAHE uses a narrower output dynamic range, yielding the lowest EME score. On the contrary, the proposed algorithm exhibits better contrast by exploiting the full dynamic range.

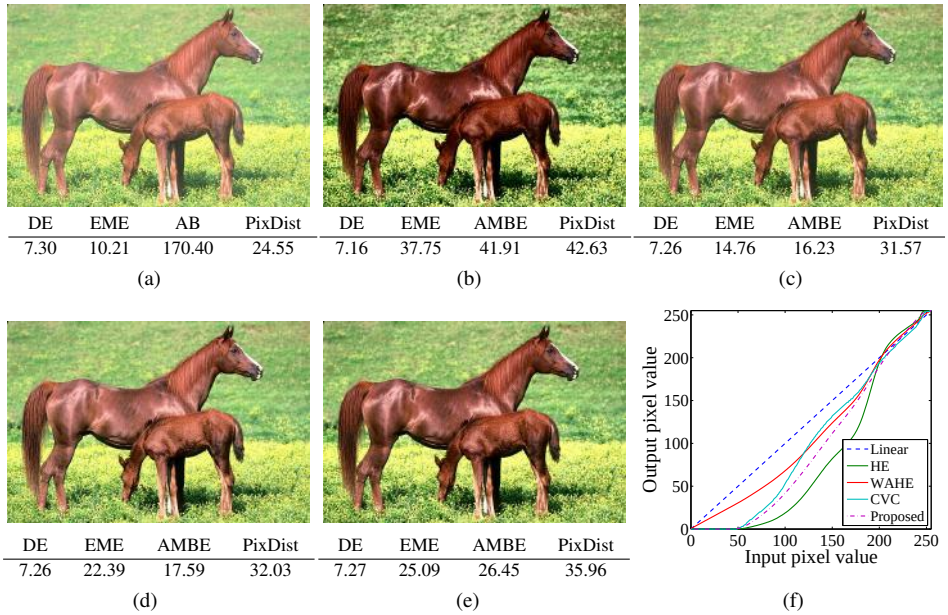

Fig. 9. CE results on the "Horse" image: (a) input image, (b) HE, (c) WAHE, (d) CVC, (e) the proposed algorithm, and (f) the comparison of the corresponding transformation functions.

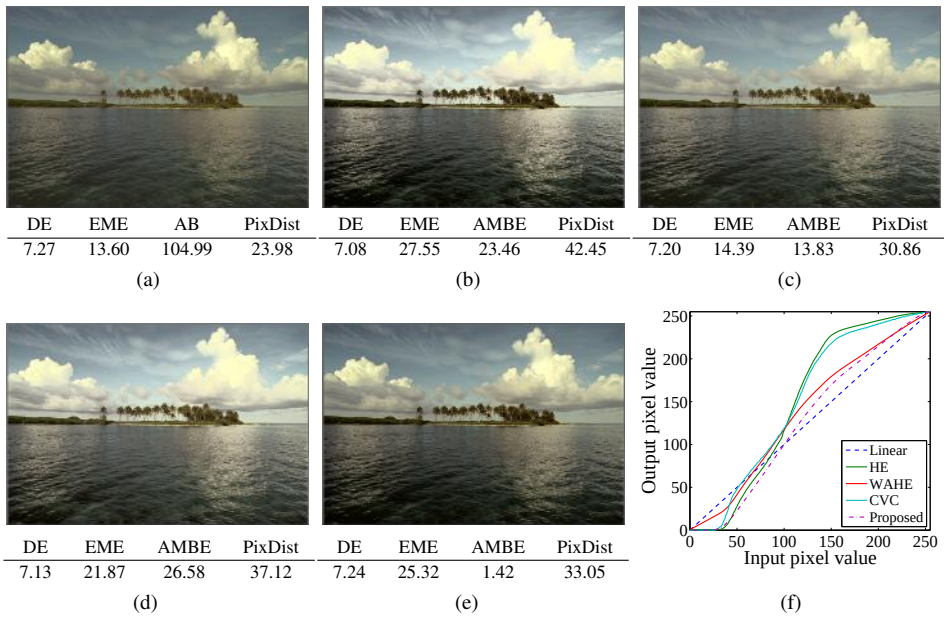

Fig. 10. CE results on the "Island" image: (a) input image, (b) HE, (c) WAHE, (d) CVC, (e) the proposed algorithm, and (f) the comparison of the corresponding transformation functions.

Fig. 9 shows the CE results on the hazy "Horse" image. HE achieves the highest EME by removing the hazy components, but it also causes the largest AMBE as it darkens pixel intensities severely. WAHE does not transform the darkest input gray-level, which is 40 in this example, to the pure black level 0. Also, WAHE transforms the input gray-levels between $[50, 100]$, which correspond to the foreground horses, with a lower increasing rate than the linear function. Therefore, it does not enhance the details on the horses clearly. Both CVC and the proposed algorithm exploit the entire dynamic range, but the proposed algorithm amplifies the gray-level differences within the horses more effectively and provides a better image quality.

In case of the "Island" image in Fig. 10, the original image looks dull due to its low contrast. HE and CVC improve the visual quality of the input image, but they incur over-enhancement problems. While they boost gray-levels within $[100, 250]$, they lose the details in the clouds and change the overall brightness dramatically from the input image. WAHE and the proposed algorithm provide comparable image qualities in this example. However, the proposed algorithm enhances the dark seawater more vividly, without losing details in the bright cloud regions.

Digital images often fail to capture scene details faithfully

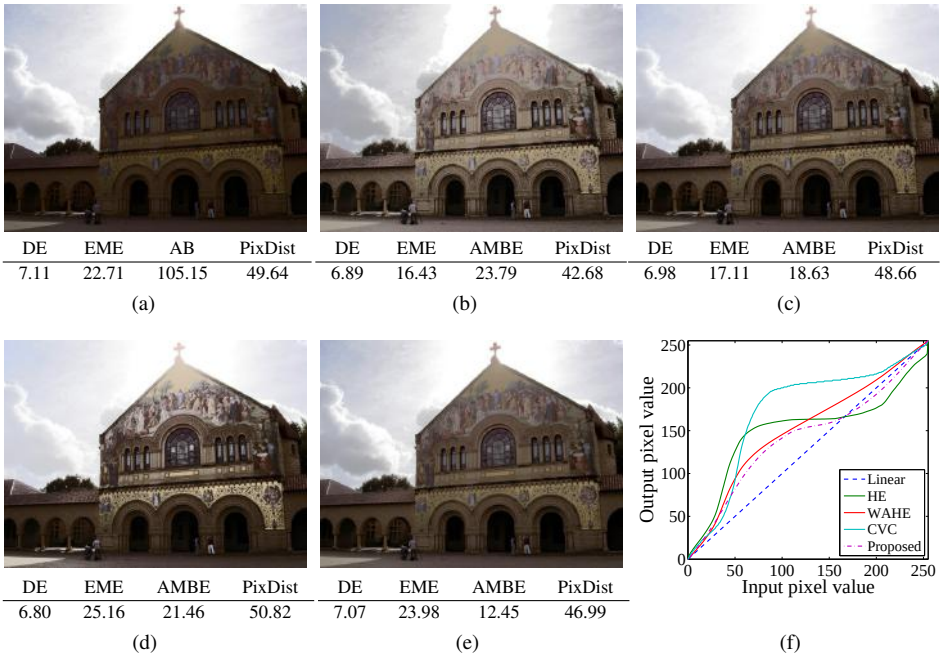

Fig. 11. CE results on the "Memorial Church" image: (a) input image, (b) HE, (c) WAHE, (d) CVC, (e) the proposed algorithm, and (f) the comparison of the corresponding transformation functions.

due to limited dynamic ranges or unideal imaging systems. In the following tests, we use test images that are acquired in those poor environments. First, most imaging systems cannot capture object details clearly when very bright and very dark regions coexist in the same scene. In such a case, an acquisition system selects the exposure setting for either bright or dark region only. Fig. 11 shows an example of a low exposure setting, which is selected to capture the bright sky area faithfully and thus degrades the details in the dark facade of the church. HE obtains the transformation function based on the 1-D histogram, without considering gray-level differences between neighboring pixels. Therefore, it over-stretches the contrast of the smooth sky region and causes contour artifacts. CVC maps input gray-levels $[30, 80]$ to output gray-levels $[50, 200]$ to enhance the contextual features such as the paintings on the wall. However, the dramatic contrast increase on this region alters the mood of the photograph undesirably. WAHE and the proposed algorithm provide more reliable CE results than HE and CVC, without the excessive alteration of the input image.

Image qualities are also degraded when scenes are captured in very low light conditions. Fig. 12 shows a dark input image, which contains noise components. When a CE algorithm boosts gray-levels indiscriminately, it also amplifies the underlying noise components. Thus, HE yields an extremely noisy image, since it transforms the darkest gray-level to 63. Although CVC exploits the 2D histogram information, it still experiences the over-enhancement problem due to the high histogram peak. WAHE suppresses the noise levels more effectively than HE and CVC, but it does not enhance the contrast sufficiently. On the other hand, the proposed algorithm alleviates the noise effects and clarifies the details of the buildings simultaneously. Therefore, the proposed algorithm provides the best subjective quality as well as the best EME score.

C. Comparison on Synthetic Images

In Fig. 13, we compare the performances of the CE algorithms on three synthetic images. The top input image with sharp edges has the same structure as Fig. 2, but it is corrupted by additive white Gaussian noise components. Therefore, we see bell shapes in the corresponding histogram. The middle input image contains a vertical gradual edge, and the bottom input image has the same edge with Gaussian noise components.

It can be observed from Fig. 13 that the proposed algorithm has the following advantages over the conventional algorithms: First, the proposed algorithm is robust against noise components. Whereas HE and CVC increase the noise variances and make each bell shape more widely distributed in the output histograms, the proposed algorithm preserves the bell shape with smaller magnification factors. Therefore, the proposed algorithm preserves homogeneous regions in an image more reliably than the conventional algorithms. Second, the proposed algorithm exploits the entire dynamic range. Given the equality constraint in (11), the proposed algorithm attempts to maximize the gray-level differences of output pixels. As a result, the proposed algorithm always transforms the darkest and the brightest pixels to the minimum and the maximum gray-levels, respectively. On the contrary, the conventional algorithms may not use the entire dynamic range, depending on the histograms of absolute gray-levels. Therefore, the proposed algorithm generally achieves higher contrast ratios than the conventional algorithms, which is confirmed by the middle and the bottom images in Fig. 13.

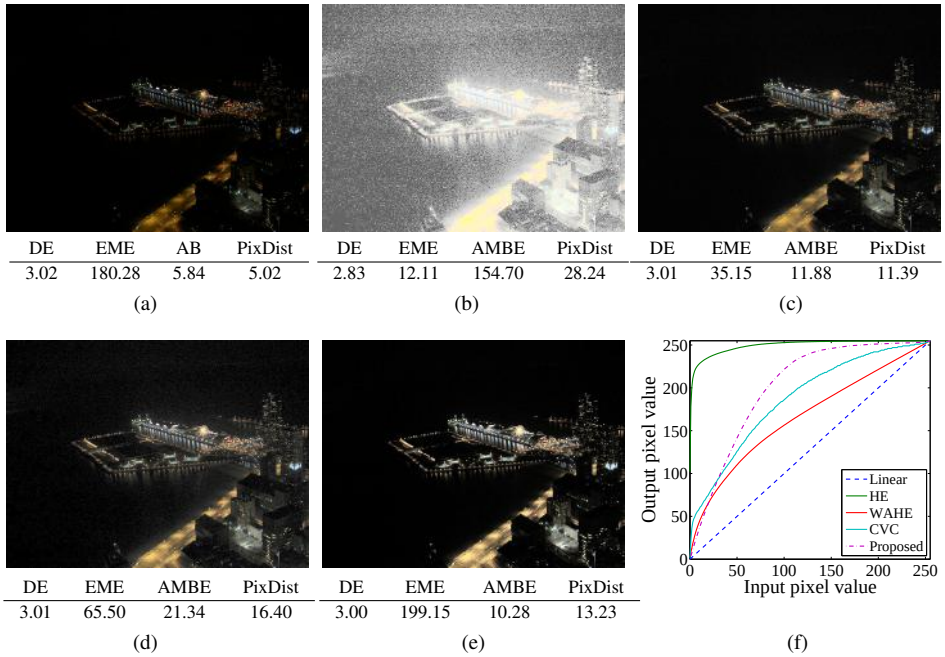

Fig. 12. CE results on the "Night View" image: (a) input image, (b) HE, (c) WAHE, (d) CVC, (e) the proposed algorithm, and (f) the comparison of the corresponding transformation functions.

D. Computation Complexity

We analyze the computational complexities of the CE algorithms to process an image of resolution $H \times W$ with K gray-levels. We divide the whole process into 3 steps: (A) the acquisition of an input histogram, (B) the modification of the histogram, and (C) the construction of the transformation function. Table II compares the computational complexities and lists the average computation times over the 600 test images. We use a personal computer with a 3.3-GHz CPU, and all algorithms are straightforwardly implemented in MATLAB without optimization.

HE and WAHE require low complexities, since they modify an acquired histogram and calculate the transformation function only once. CVC demands the highest computational burden, since it solves the matrix inverse problem to obtain the desired 2D histogram. Moreover, CVC adopts the block-based acquisition and processing of the 2D histogram information, and its complexity is proportional to the block size w^2. Notice that the proposed algorithm is much simpler than CVC, although both algorithms are based on the 2D histogram information. The proposed algorithm takes only 29 ms to process an image on average.

V. Conclusions

We proposed a novel contrast enhancement algorithm using the LDR, in which the statistical information of gray-level differences between neighboring pixels in an input image is exploited to control output gray-level differences. We observed that frequently occurring gray-level differences should be amplified to enhance the contrast of the output image, and then formulated the CE as a constrained optimization problem. The proposed algorithm consists of two main steps. First, the intra-layer optimization obtains the difference vector at each layer by solving the constrained optimization problem. Second, the inter-layer aggregation combines the difference vectors at all layers into the unified difference vector, which is equivalent to the transformation function. Extensive experimental results demonstrated that the proposed algorithm provides better image qualities than the conventional algorithms.

References

[1] C. Lee, C. Lee, and C.-S. Kim, "Contrast enhancement based on layered difference representation," in *Proc. IEEE ICIP*, Sep.–Oct. 2012, pp. 965–968.

[2] D. Jobson, Z. Rahman, and G. Woodell, "Properties and performance of a center/surround retinex," *IEEE Trans. Image Process.*, vol. 6, no. 3, pp. 451–462, Mar. 1997.

[3] G. Deng, "A generalized unsharp masking algorithm," *IEEE Trans. Image Process.*, vol. 20, no. 5, pp. 1249–1261, May 2011.

[4] S. M. Pizer, E. P. Amburn, J. D. Austin, R. Cromartie, A. Geselowitz, T. Greer, B. ter Haar Romeny, J. B. Zimmerman, and K. Zuiderveld, "Adaptive histogram equalization and its variations," *Comput. Vis. Graph. Image Process.*, vol. 39, no. 3, pp. 355–368, Sep. 1987.

[5] J. Stark, "Adaptive image contrast enhancement using generalizations of histogram equalization," *IEEE Trans. Image Process.*, vol. 9, no. 5, pp. 889–896, May 2000.

[6] J.-Y. Kim, L.-S. Kim, and S.-H. Hwang, "An advanced contrast enhancement using partially overlapped sub-block histogram equalization," *IEEE Trans. Circuits Syst. Video Technol.*, vol. 11, no. 4, pp. 475–484, Apr. 2001.

[7] R. C. Gonzalez and R. E. Woods, *Digital Image Processing*, 3rd ed. Prentice Hall, 2007.

[8] Y.-T. Kim, "Contrast enhancement using brightness preserving bi-histogram equalization," *IEEE Trans. Consum. Electron.*, vol. 43, no. 1, pp. 1–8, Feb. 1997.

[9] Y. Wang, Q. Chen, and B. Zhang, "Image enhancement based on equal area dualistic sub-image histogram equalization method," *IEEE Trans. Consum. Electron.*, vol. 45, no. 1, pp. 68–75, Feb. 1999.

[10] S.-D. Chen and A. Ramli, "Minimum mean brightness error bi-histogram equalization in contrast enhancement," *IEEE Trans. Consum. Electron.*, vol. 49, no. 4, pp. 1310–1319, Nov. 2003.

[11] Q. Wang and R. K. Ward, "Fast image/video contrast enhancement based on weighted thresholded histogram equalization," *IEEE Trans. Consum. Electron.*, vol. 53, no. 2, pp. 757–764, May 2007.

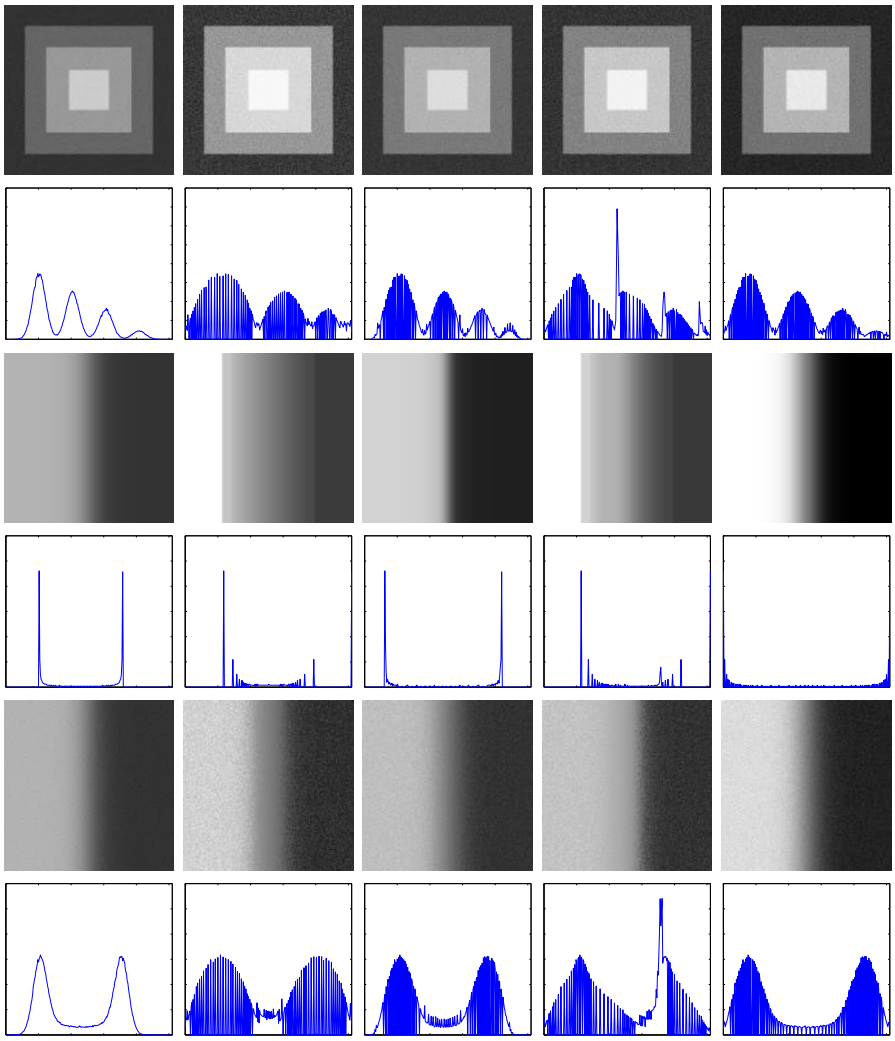

Fig. 13. CE results on three synthetic images. The first, third, and fifth rows correspond to the input and output images, and the other rows show the corresponding histograms of the upper images. (a) Input. (b) HE. (c) WAHE. (d) CVC. (e) Proposed.

TABLE II
ANALYSIS OF THE COMPUTATIONAL COMPLEXITIES OF THE CE ALGORITHMS. H AND W DENOTE THE HEIGHT AND THE WIDTH OF AN INPUT IMAGE, AND K IS THE NUMBER OF GRAY-LEVELS. ALSO, w^2 IN CVC DENOTES THE BLOCK SIZE IN ITS BLOCK-BASED PROCESSING.

	HE	WAHE	CVC	Proposed
A: Histogram acquisition	$\mathcal{O}(HW)$	$\mathcal{O}(HW)$	$\mathcal{O}\left(w^2HW\right)$	$\mathcal{O}(HW)$
B: Histogram modification	-	$\mathcal{O}(K)$	$\mathcal{O}(K^2)$	$\mathcal{O}(K^2)$
C: Mapping construction	$\mathcal{O}(K)$	$\mathcal{O}(K)$	$\mathcal{O}(K^3)$	$\mathcal{O}(K^2)$
Total	$\mathcal{O}(HW+K)$	$\mathcal{O}(HW+K)$	$\mathcal{O}(w^2HW+K^3)$	$\mathcal{O}(HW+K^2)$
Computation Times (ms)	7.3	17.5	7865.0	29.0

[12] C. Lee, C. Lee, Y.-Y. Lee, and C.-S. Kim, "Power-constrained contrast enhancement for emissive displays based on histogram equalization," *IEEE Trans. Image Process.*, vol. 21, no. 1, pp. 80–93, Jan. 2012.

[13] S. Naik and C. Murthy, "Hue-preserving color image enhancement without gamut problem," *IEEE Trans. Image Process.*, vol. 12, no. 12, pp. 1591–1598, Dec. 2003.

[14] J.-H. Han, S. Yang, and B.-U. Lee, "A novel 3-D color histogram equalization method with uniform 1-D gray scale histogram," *IEEE Trans. Image Process.*, vol. 20, no. 2, pp. 506 –512, Feb. 2011.

[15] E. Hadjidemetriou, M. Grossberg, and S. Nayar, "Multiresolution histograms and their use for recognition," *IEEE Trans. Pattern Anal. Mach. Intell.*, vol. 26, no. 7, pp. 831–847, Jul. 2004.

[16] T. Arici, S. Dikbas, and Y. Altunbasak, "A histogram modification framework and its application for image contrast enhancement," *IEEE Trans. Image Process.*, vol. 18, no. 9, pp. 1921–1935, Sep. 2009.

[17] T. Celik and T. Tjahjadi, "Contextual and variational contrast enhancement," *IEEE Trans. Image Process.*, vol. 20, no. 12, pp. 3431–3441, Dec. 2011.

[18] J. DiCarlo and B. Wandell, "Rendering high dynamic range images," in *Proc. SPIE*, vol. 3965, May 2000, pp. 392–401.

[19] R. Fattal, D. Lischinski, and M. Werman, "Gradient domain high dynamic range compression," *ACM Trans. Graph.*, vol. 21, pp. 249–256, Jul. 2002.

[20] C. Wang, J. Peng, and Z. Ye, "Flattest histogram specification with accurate brightness preservation," *IET Image Process.*, vol. 2, no. 5, pp. 249–262, Oct. 2008.

[21] J. Gross and J. Yellen, *Graph Theory and Its Applications*, 2nd ed. Chapman & Hall, 2006.

[22] C. L. Lawson and R. J. Hanson, *Solving Least Squares Problems*. SIAM, 1974.
[23] J. Nocedal and S. J. Wright, *Numerical Optimization*, 2nd ed. Springer, 2006.
[24] R. Baraniuk, "Compressive sensing," *IEEE Signal Process. Mag.*, vol. 24, no. 4, pp. 118–121, Jul. 2007.
[25] E. Candés and T. Tao, "Decoding by linear programming," *IEEE Trans. Inf. Theory*, vol. 51, no. 12, pp. 4203–4215, Dec. 2005.
[26] *Kodak Lossless True Color Image Suite*, 2013 [Online]. Available: http://r0k.us/graphics/kodak/.
[27] *USC-SIPI database* [Online]. Available: http://sipi.usc.edu/database/.
[28] P. Arbelaez, M. Maire, C. Fowlkes, and J. Malik, "Contour detection and hierarchical image segmentation," *IEEE Trans. Pattern Anal. Mach. Intell.*, vol. 33, no. 5, pp. 898–916, May 2011.
[29] C. E. Shannon, "A mathematical theory of communication," *Bell Syst. Tech. J.*, vol. 27, pp. 379–423, 623–656, Jul. Oct. 1948.
[30] S. Agaian, B. Silver, and K. Panetta, "Transform coefficient histogram-based image enhancement algorithms using contrast entropy," *IEEE Trans. Image Process.*, vol. 16, no. 3, pp. 741–758, Mar. 2007.
[31] Z. Chen, B. R. Abidi, D. L. Page, and M. A. Abidi, "Gray-level grouping (GLG): An automatic method for optimized image contrast enhancement–Part I: The basic method," *IEEE Trans. Image Process.*, vol. 15, no. 8, pp. 2290–2302, Aug. 2006.
[32] T. Cover and J. Thomas, *Elements of Information Theory*, 2nd ed. Wiley–Interscience, 2006.

Chulwoo Lee (S'11) received the B.S. degree in the School of Electrical Engineering from Korea University, Seoul, Korea, in 2008, where he is currently pursuing the Ph.D. degree in electrical engineering. His research interests include power-constrained image processing, contrast enhancement, and computer vision.

Chul Lee (S'06-M'13) received the B.S., M.S., and Ph.D. degrees from the School of Electrical Engineering, Korea University, Seoul, Korea, in 2003, 2008, and 2013, respectively. From 2002 to 2006, he was with Biospace Inc., Seoul, Korea, where he was with the development of medical equipment. He is currently a Postdoctoral Scholar with the Department of Electrical Engineering, The Pennsylvania State University, University Park, PA, USA. His current research interests include image restoration, power-constrained contrast enhancement, and high dynamic range imaging.

Chang-Su Kim (S'95-M'01-SM'05) received the Ph.D. degree in electrical engineering from Seoul National University (SNU), Seoul, Korea, with a Distinguished Dissertation Award in 2000. From 2000 to 2001, he was a Visiting Scholar with the Signal and Image Processing Institute, University of Southern California, Los Angeles, CA, USA. From 2001 to 2003, he coordinated the 3-D Data Compression Group, National Research Laboratory for 3-D Visual Information Processing, SNU. From 2003 and 2005, he was an Assistant Professor with the Department of Information Engineering, Chinese University of Hong Kong, Hong Kong. In September 2005, he joined the School of Electrical Engineering, Korea University, Seoul, Korea, where he is currently a Professor. His current research interests include image processing and multimedia communications. In 2009, he received the IEEK/IEEE Joint Award for Young IT Engineer of the Year. He has published more than 200 technical papers in international journals and conferences. He is an Editorial Board Member of the *Journal of Visual Communication and Image Representation* and an Associate Editor of the IEEE TRANSACTIONS ON IMAGE PROCESSING.